

A Microresonator Based Laser Velocity Sensor

Benjamin J. A. Wise ^{*}, Vahid Eghbalifarkoosh ^{*}, and M. Volkan Ötügen [†]

Southern Methodist University, Dallas, TX 75205, USA

Dominique Fourquette [‡]

Michigan Aerospace Corporation, Ann Arbor, MI 48108, USA

A laser velocity sensor concept based on optical microresonators is presented. In the present paper the application to spacecraft atmospheric entry is explored. The concept is based on the measurement of Doppler shift of back-scattered laser light. Specifically, the Doppler shift is detected by observing the whispering gallery optical modes (WGM) of a dielectric microresonator excited by the back scattered light from particulates and gas molecules. The microresonator replaces the typical Fabry-Perot interferometer, thereby significantly reducing the size and weight of the overall detection system. This paper presents proof-of-concept results. The Doppler shift of a tunable narrow line laser scattered from the edge of a rotating disk is measured using a $\approx 500\mu\text{m}$ diameter silica sphere. These preliminary results indicate that such a detection scheme is possible although improvements to signal processing may be required for measurements in a gas.

Nomenclature

l	Integer number of wavelengths
n_0	Index of refraction of microresonator
Q	Optical quality factor
r	Radius of microresonator
t	Time
λ	Vacuum wavelength of light
λ_{Center}	Center wavelength of Laser scan
$\delta\lambda$	Linewidth of transmission “Dips”
$\Delta\lambda_{Doppler}$	Change in λ due to Doppler shift
$\Delta\lambda_{Measured}$	Measured change in λ

I. Introduction

The main motivation of the present velocity measurement concept is the need for accurate speed measurements during atmospheric entry of spacecraft. For example, during the entry, descent, and landing (EDL) phase of Mars Missions – or for that matter any atmospheric EDL – accurate information on vehicle velocity, altitude, and attitude are critical for success of the EDL operation.

This fact has been most recently demonstrated by the crash of the Schiaparelli module (Entry Demonstrator Module or EDM) of the European Space Agency’s ExoMars 2016 Mission. The Schiaparelli crash was caused primarily by sensor failure and faulty logic in reconciling measurements between the Radar Doppler Altimeter (or RDA, which was operating nominally) and the Inertial Measurement Unit (or IMU, which had become saturated and was producing a faulty signal).¹ The total dependence of the lander on the IMU

^{*}Graduate Research Assistant, Mechanical Engineering, Bobby B. Lyle School of Engineering, 3101 Dyer Street, Room 215, Dallas, TX 75205, and AIAA Student Member.

[†]Senior Associate Dean of Engineering and Professor of Mechanical Engineering, Bobby B. Lyle School of Engineering, 3101 Dyer Street, Room 105E, Dallas, TX 75205, and AIAA Associate Fellow.

[‡]Vice President of R&D, 1777 Highland Drive, Ann Arbor, MI 48108, and AIAA Associate Fellow.

for all but the terminal 106 seconds of the mission and the lack of redundancy and error checking in the measurement — faulty measurements from the IMU continued to be used for the duration of the mission, even after the IMU saturation flag was raised — were critical design errors that led to the total loss of the EDM.¹

With the increasing complexity of EDL operations, accurate and near real time measurements of a lander’s airspeed during entry, descent, and landing, as well as altitude and attitude (measured by complementary instruments), increases the likelihood of mission successes, which, as demonstrated by the Schiaparelli module, can often hinge on the accuracy (and fault-free operation) of only one sensing instrument. While fully integrated and tested devices for direct optical measurement of airspeed are commercially available,² many are too bulky and far too heavy to be feasible for planetary exploration and other high speed applications.

In this paper, we discuss utilizing Whispering Gallery Mode (WGM) based optical microresonators³ as a possible replacement for the bulky and heavy Fabry-Perot interferometers common in a range of other direct optical airspeed sensors, such as LIDAR systems, which will allow the miniaturization and weight reduction of these sensing systems to make them feasible for planetary exploration. We also present preliminary data to demonstrate that, at the proof of concept level, Doppler shift measurement with WGM based sensors is possible, and can provide high resolution velocity information.

II. Measurement Principle

A. The Whispering Gallery Mode

The measurement principle of a WGM based microresonator is similar to that of a Fabry-Perot interferometer, with a few, mainly geometric, exceptions. One of the most immediate differences is the cavity shape. The WGM based microresonators are spherical (rather than linear or confocal for most Fabry-Perot interferometers), but may also be cylindrical, disk-shaped, or toroidal in nature.³ The optical path must remain close to tangential — or more accurately, the optical path must make an angle smaller than the critical angle with the surface — in order to ensure that light in the cavity experiences total internal reflection and remains trapped inside the sphere.

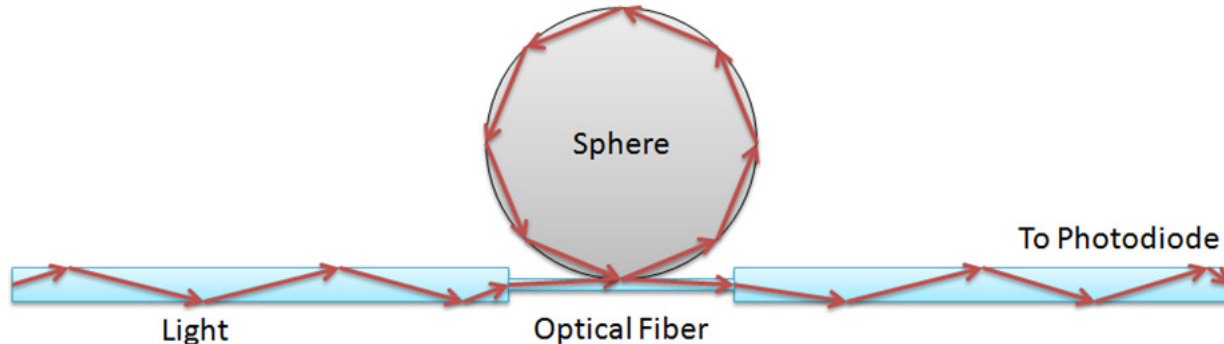


Figure 1. Fiber Coupled WGM Microresonator

Figure 1 shows, schematically, a typical fiber coupled WGM microresonator configuration. Laser light is coupled into the sphere through the optical fiber (or another type of waveguide) at grazing angle. When the light returns to its entry point exactly in phase, an optical resonance is observed. We can estimate the optical resonance condition to be

$$2\pi r n_0 = l\lambda \quad (1)$$

which holds for $r \gg \lambda$. When the light from the laser is tuned across a narrow range, the optical WGM resonances are excited each time the condition of Equation 1 is met. The WGM are observed as sharp dips in the transmission spectrum by a photodetector placed on the other end of the fiber. Each dip in the transmission spectra corresponds to a different integer value of the circumferential mode number, l , in Equation 1.

The fact that light is coupled into the WGM microresonator tangentially and remains in the resonator via total internal reflection, rather than just the high reflectivity and/or anti-reflective coatings of Fabry-Perot interferometer components, means that the resonator itself has very low optical loss. The losses in a given resonator are described in terms of, Q , the optical quality factor, which is a ratio of energy stored to energy lost, such that as losses vanish, $Q \rightarrow \infty$. The linewidth of the observed resonances, $\delta\lambda$, which directly impacts the measurement resolution, is related to the Q -factor shown as

$$Q = \frac{\lambda}{\delta\lambda} \quad (2)$$

The reason WGM microresonators in this configuration are so remarkable, and why they show so much promise for planetary exploration and high velocity flow applications, are the unusually high Q -factors we can achieve (in excess of 10^7 is routinely achieved by our lab, with maximal values greater than 10^9 for select applications), while maintaining a remarkably small physical size and low mass.⁴

High optical quality factor dielectric microspheres have received significant attention for their potential application in a wide range of fields. WGM applications have been explored in communication (switching, filtering, and multiplexing) and sensor technologies.⁵ Sensors utilizing the whispering gallery mode (WGM) shifts of microspheres have been proposed for impurity detection in liquids,⁶ mechanical sensing, including force,⁴ pressure,⁷ temperature,⁸ and wall shear stress for aerodynamic applications,⁹ as well as, electric¹⁰ and magnetic field strength measurement.^{11,12}

B. Doppler Shift Measurement

In the present application, we shine a narrow line-width tuneable laser at a target, collect scattered light, and couple it into a microresonator. The collected light is first coupled into a single mode fiber and then side-coupled into the microresonator in a similar fashion to that depicted in Figure 1. The only difference is that light scattered from a target travels through the fiber rather than the laser light itself. We observe the WGM as a series of troughs through the transmission spectra (photodiode output) as we tune the narrow-line interrogation laser. The WGM shifts in the spectra, relative to a reference spectrum taken while the target is stationary, are proportional to the Doppler shift of the scattered light from the target. In the atmospheric application, the scattering is expected to be a combination of Mie (scattering from particulates in the atmosphere) and Rayleigh (molecular scattering from small particulates and gas molecules). In the present phase of the study, as a first order proof of concept, we measure the rotational speed of a disk using a low power, narrow line, tunable Littman-Metcalf cavity diode laser as the light source.¹³

III. Experiments

A. Experimental Setup

In these experiments, we demonstrate the detection of Doppler shifts of light scattered from a (solid) moving target as a proof of concept. In order to take advantage of the high WGM Q -factors of our microresonators and detect small Doppler shifts, we use a narrow linewidth laser aimed at a target location and in the desired measurement direction. The scattered light from the target location is collected and fed (via side coupling) into the microresonator. As the laser frequency is tuned over a narrow range, the optical modes (WGM) of the resonator are excited by the surface-scattered light. The fiber serves as an input-output device, and is connected to a free space to fiber coupler on one end and a photodiode on the other. The WGM are observed as dips in the transmission spectrum through the fiber. The shifts of these WGM relative to a reference indicate the Doppler shift of the collected light which can be related to the relative speed of the target.

The experimental setup (Figure 2) is designed to show that the WGM microresonator-based velocity sensor is capable of measuring Doppler shift from scattered laser light. We use the edge of a spinning hard drive disk as the moving target. The laser beam from a 9mW, 639nm Littman-Metcalf cavity diode laser (New Focus Vortex TLB 6800, with a line width of 200 kHz), is focused on the edge of the rotating disk. Disk angular velocities ranged between 60–240 rotations per second (corresponding to edge tangential velocities of 15–75 m/s). Doppler-shifted scattered light is collected with a certain cone angle, collimated, and subsequently reduced in diameter to couple it into a single mode optical fiber as shown in Figure 2. The core diameter of the SM fiber is $1\mu\text{m}$.

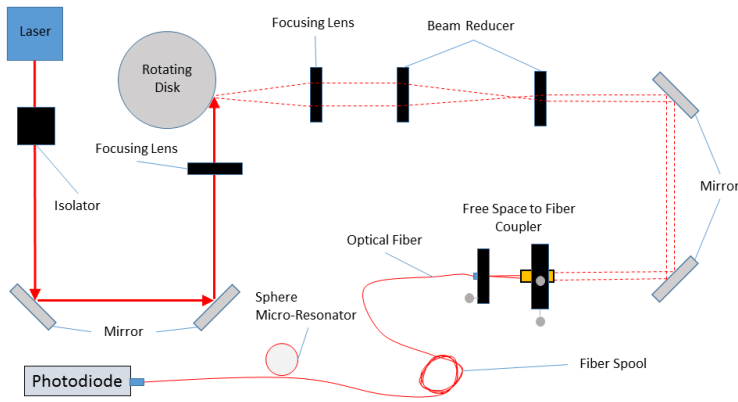


Figure 2. Experimental Setup (Schematic)

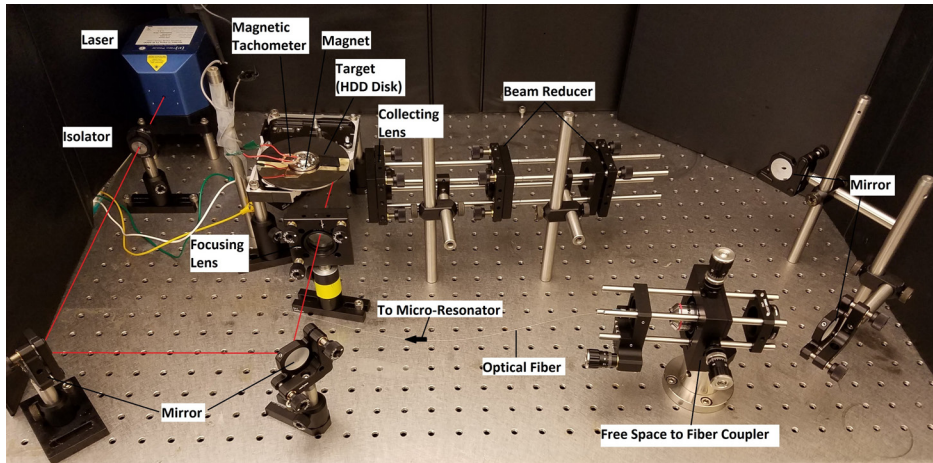


Figure 3. Experimental Setup

The fiber coupled light is then directed through a tapered section of fiber, where it is coupled into a spherical silica microresonator, with diameter $\approx 500\mu\text{m}$, acting as an ultra-high resolution interferometer. The transmitted light is detected by a photodetector (ThorLabs PD36A) and its output is discretized by a 16 bit analog-to-digital converter. The data is stored and analyzed on a desktop computer. A photograph of the setup is shown in Figure 3. A magnetic tachometer is used to accurately determine the rotational frequency of the disk. Figure 4 is a photograph of the microsphere resonator and the coupling fiber. The lasers nominal output power is 9 mW and approximately 1.6 mW of light scattered from the disk edge is captured by the collecting optics. From this, about $13.5\ \mu\text{W}$ of the light is coupled into the SM optical fiber (before tapering). The amount of light detected by the photodetector (after fiber tapering) during the measurements is $0.05\ \mu\text{W}$. Clearly, optical coupling efficiency at the various stages is a challenge in the present system.

B. Results

Using the setup described above, a set of experiments were performed with different disk rotational speeds. A summary of these preliminary results is presented in Figures 5 and 6.

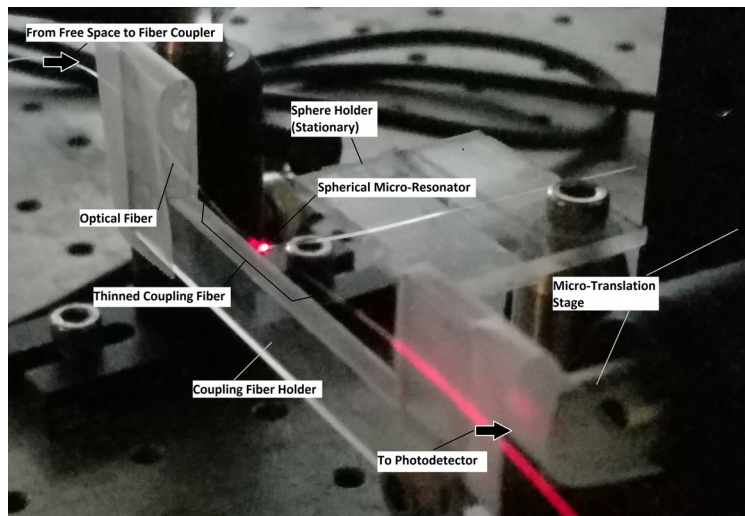


Figure 4. Fiber-Microresonator Coupling

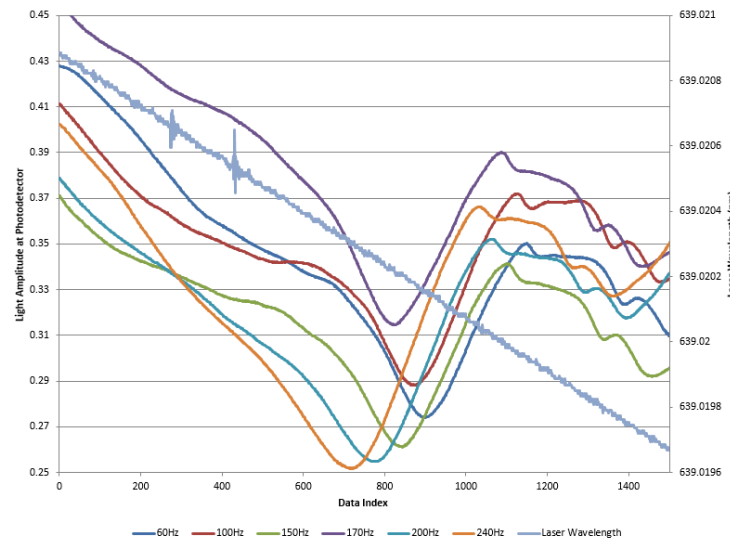


Figure 5. Transmission Spectrum around Selected WGM Dip

The laser was scanned at a rate of 700 Hz (using a ramp/triangle waveform). Across each scan of the laser, 6000 digitized data points were recorded to form the transmission spectra. Figure 5 shows a subrange in the transmission spectra that captures a single WGM at various disk frequencies, along with the corresponding laser wavelength (negative ramp signal). As the disk's rotational frequency increases, the WGM moves to the left (longer wavelengths) due to Doppler shift. The curve for each disk frequency shown in the figure is an ensemble average of approximately 600 successive scans of the laser. Due to photon shot noise (weak light power incident on the photodetector) and the wobbling of the disk (which results in variable signal strength and signal dropout through each revolution of the disk), it was not possible to discern WGM of the microsphere through the transmission spectrum from each individual scan of the laser alone. Thus, ensemble averaged transmission spectra are used to determine the WGM and the Doppler shifts. The total duration for each measurement is on the order of a second. Note that the light amplitude at the photodetector is in arbitrary units, due to the variance of light levels for subsequent scans caused by the disk's beam steering.

Figure 6 shows WGM shifts (corresponding to the Doppler shifts) of the data of Figure 5. This figure

presents three different approaches of determining dip location, along with the least squares regressions for each resonance shift detection method.

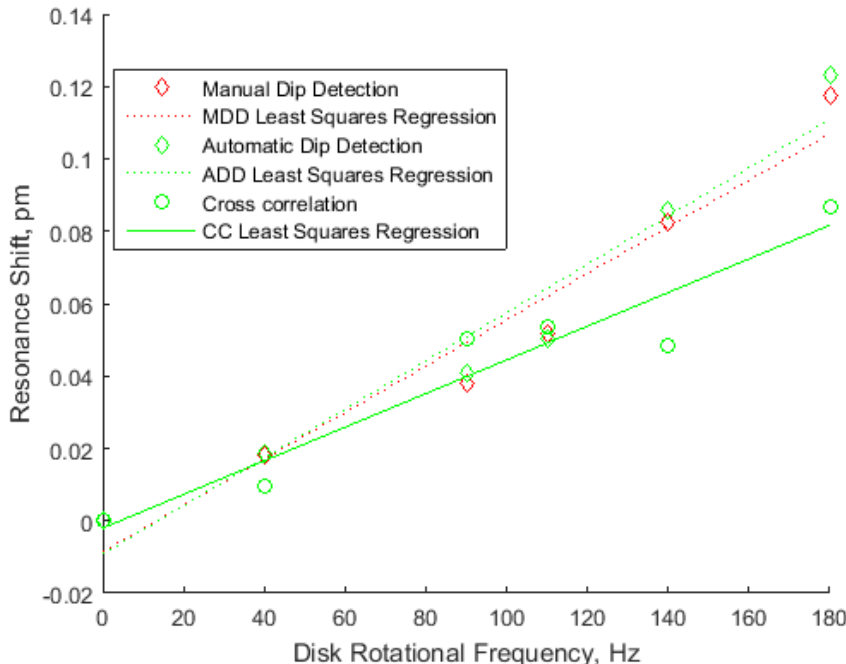


Figure 6. WGM Shift vs Disk Rotational Frequency for Data of Figure 5

In the manual dip detection (MDD) method, WGM shifts are determined manually (or visually) by selecting the location of the minimum value of each dip. The automatic dip detection (ADD) method uses software to choose the absolute minimum value in each data vector (ensemble averaged scan), which is much faster than MDD, but may be challenged by noisy data. In the last method, cross-correlation (CC) is performed between each data vector and a reference data vector. There is good agreement between MDD and ADD results. The CC results show slightly lower Doppler shifts and have a larger scatter, which perhaps indicates that further signal processing and/or an increased number of resonance features are required to allow a more robust cross-correlation approach. Cross-correlation approach generally is preferable to the ADD method, given that it is less susceptible to noisy data, and can be computationally less demanding.

Spline fitting of the resonance dips was also attempted and produced accurate results for individual resonance centers. However, programmatic limitations of automatic spline fitting to order five or less restrict their use to single resonances, whereas the CC method can analyze an entire scan (and tends to produce more accurate results using signals containing multiple resonances). Though spline fitting of resonances is a tenable avenue of signal processing for this experiment (and will be explored further in future systems), for the moment, cross-correlation is the preferred method for shift detection given its ability to analyze whole scans without human interaction and with relatively low computational effort.

C. Signal Processing

As discussed in the previous sections, we experienced signal degradation and dropout caused by the wobble in disk rotation. The problem is especially acute due to the high precision required in free space-to-single mode fiber coupling. On the other hand, the experiment allows for a realistic test of the measurement approach for the Mie scattering regime and in cases where there is beam steering due to atmospheric turbulence. Clearly, a more robust signal processing method, in conjunction with the physical design improvement are required in order to increase the reliability of the measurement system. Figure 7 shows three different raw (single) scans from the same data set, taken no more than a few milliseconds apart. In orange we see what a typical WGM spectrum looks like, a fairly complex signal with many distinct peaks and valleys of

transmission, in blue we see a scan that potentially has some interesting information, particularly between indices 6000 and 8000, but otherwise appears to be mostly background noise, and in green we see a spectrum that is almost completely background noise. These are three of the 600 scans collected for a given disk speed. Some scans contain excellent information, some contain intermittent information, and some contain little or no information.

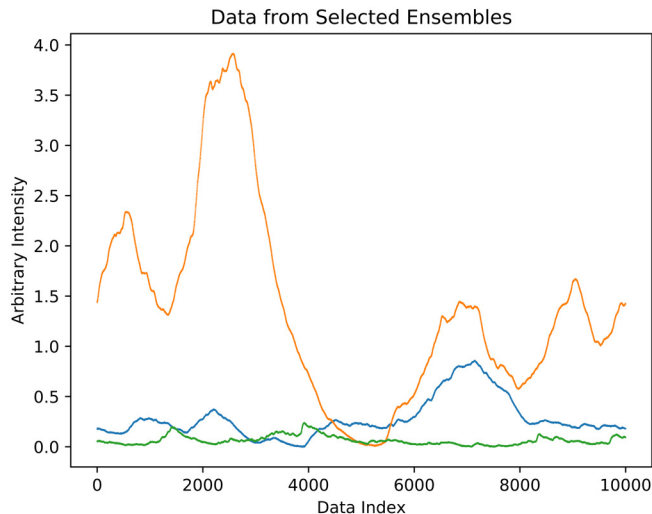


Figure 7. Signal Processing Motivation - Selected Scans

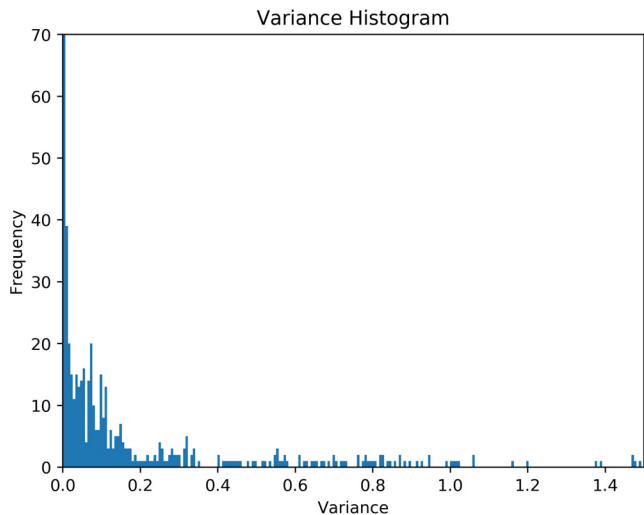


Figure 8. Signal Processing Motivation - Histogram

For the results shown in the previous section (Figure 5), the only data processing done is phase locked averaging of the 600 individual scans to obtain an ensemble of the transmission spectrum at a given disk speed. We then compare this ensemble (either manually or via cross-correlation) to a previous measurement to determine the shift in wavelength of the resonances, and finally, via calibration of the laser we relate this shift to some change in the quantity we want to measure. Clearly, with an intermittent signal such as this one, this approach may not be sufficient for reliable measurements.

Observing Figure 7, the scans with no or small portion of signal dropout (orange trace), have strong features in the transmission spectrum, hence have large variance (mean square). Analysis of the variances of all 600 scans in one data set (disk speed) is shown in Figure 8 in the form of a histogram. A large number of scans show very low variance, so much so that the first bin in Figure 8 has over three times more scans than any other bin. We hypothesize that by choosing only high variance scans for use in our ensemble averaging, our signal to noise ratio would improve, resulting in signals that are better suited for cross-correlation. Along, with this filter, which can be set by introducing a cut-off variance below which a scan is discarded, we can likely reduce the stochastic error by taking a large number of scans and ensemble-averaging them in order to mitigate signal dropout without degrading essential spectral information.

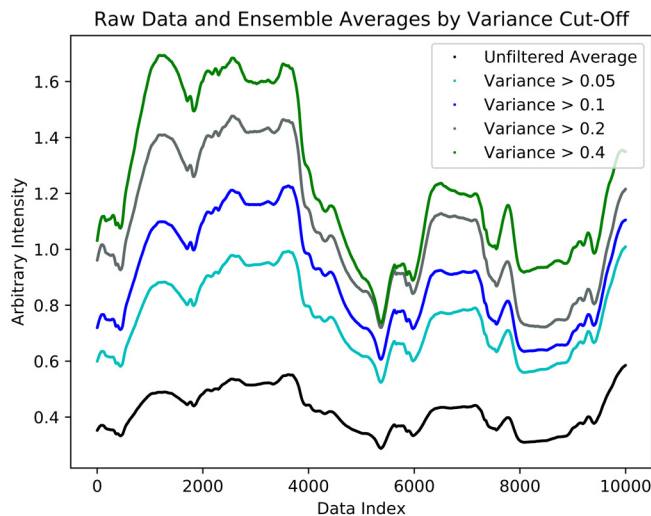


Figure 9. Signal Processing Results

Figure 9 shows the unfiltered ensemble average in black, and various filtered ensemble averages in different colors. The figure offers interesting observations: Firstly, features are increasingly crisp and more distinct as the cut-off variance is increased. Additionally, we can see the signals beginning to converge on certain points in the spectrum, e.g. around index 5500, which indicates that a cut-off variance of around that level allows for good signal agreement, while removing noise contributed by signal dropout.

IV. Free Space Coupling

In previous sensor development efforts, such as the E- and B-Field sensors¹⁰ and the seismometer,¹⁴ our optical sensors have always utilized direct fiber coupling, as in Figures 1 and 4, which resulted in a coupling signal that was stable in time with respect to the stability of the laser diode. However, in the experiment discussed above, we experienced intermittent signal loss (drop out) due to coupling scattered light into a single mode fiber with a very small numerical aperture, shown in Figure 7 and 8.

A. Experimental Setup

In order to make our sensor design more robust, we carried out an additional experiment in which we free space couple the light into the resonator, as shown in Figure 10 and 11, and observe the WGMs through scattering from the sphere instead of transmission through the coupling fiber. In this preliminary test, we focus the laser light on to the side of the sphere resonator and capture the light scattered from the sphere, which is directed onto a photo-detector, as shown in Figure 10. A portion of the scattered light should be from that coupled into the sphere tangentially. Therefore, as the laser frequency is scanned the WGMs of the sphere should be observed in the scattered light.

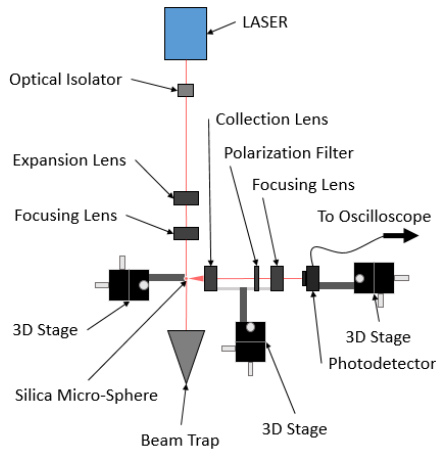


Figure 10. Schematic of Experiment

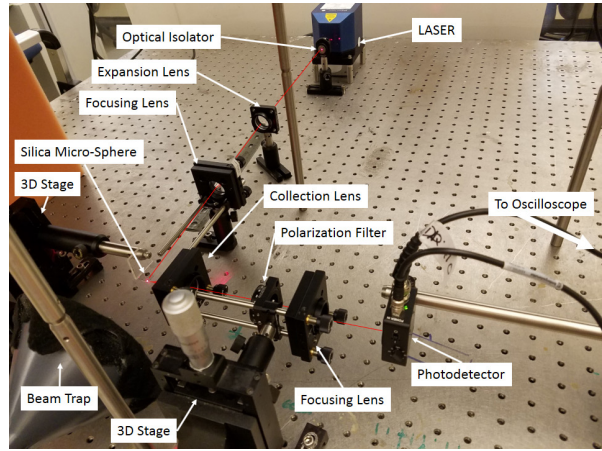


Figure 11. Experimental Setup

B. Results

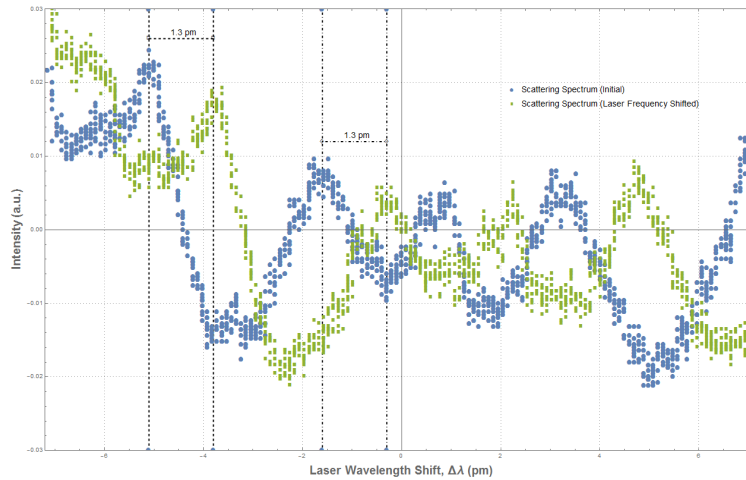


Figure 12. Results

Figure 12 demonstrates that using a silica microsphere excited via free space laser light as described above, we can detect a shift in the wavelength of the light irradiating the sphere by observing the shift in the WGM in scattered light. The figure shows the resonance spectrum (in blue). Additionally, in Figure 12 we have imposed a shift, $\Delta\lambda = 1.3\text{pm}$, on the center wavelength of the interrogation laser (simulating a Doppler shift), which is responsible for the laser frequency shifted scattering spectrum (green). Therefore, in principle, Doppler shift measurements can be made using free space coupling of scattered light into the resonator.

V. Conclusion

These preliminary results are encouraging. In the first phase of this project we were able to demonstrate the measurement of Doppler-shift of laser light scattered from a moving target using a dielectric microresonator side-coupled to a single mode optical fiber. Also, we note that due to the high optical quality factors possessed by the microresonators, very small changes in the target velocity can be determined. For example, the current preliminary results indicate that, for a back-scatter LIDAR system using a side-coupled WGM

resonator, a velocity resolution of 2.4 m/s is possible. Signal processing that selects scans with variances over a certain threshold value can at least partially mitigate the signal dropout effects when using fiber coupled approach. Another possible approach to mitigate signal dropout due to beam steering may be direct (free space) coupling of scattered light into the optical resonator and observing the WGMs in the light scattered from the resonator.

Acknowledgments

We gratefully acknowledge the support of NASA through SBIR Phase I and II contracts, No.: NNX17CL10C, with Dr. Farzin Amzajerdian as Program Manager. The authors would also like to thank Sujoy Purkayastha for assistance with this research.

References

- ¹ESA Inspector General Tolker-Nielsen, T., “EXOMARS 2016 - Schiaparelli Anomaly Inquiry,” Tech. rep., European Space Agency, 2017.
- ²“AeroForecast (R) Optical Air Data System,” 2017.
- ³Matsko, A. and Ilchenko, V., “Optical resonators with whispering-gallery modes-part I: basics,” *IEEE journal of selected topics in quantum electronics a publication of the IEEE Lasers and Electro-optics Society.*, Vol. 12, No. 3, 2006, pp. 3–14.
- ⁴Ioppolo, T., Kozhevnikov, M., Stepaniuk, V., Otugen, M. V., and Sheverev, V., “Micro-optical force sensor concept based on whispering gallery mode resonators,” *Applied Optics*, Vol. 47, No. 16, 2008, pp. 3009.
- ⁵Matsko, A. B., Savchenkov, A. A., Strekalov, D., Ilchenko, V. S., and Maleki, L., “Review of Applications of Whispering-Gallery Mode Resonators in Photonics and Nonlinear Optics,” 2005.
- ⁶Ioppolo, T., Das, N., and Otugen, M. V., “Whispering gallery modes of microspheres in the presence of a changing surrounding medium: A new ray-tracing analysis and sensor experiment,” *Journal of Applied Physics*, Vol. 107, No. 10, 2010, pp. 103105.
- ⁷Ioppolo, T. and Otugen, M. V., “Pressure tuning of whispering gallery mode resonators,” *J. Opt. Soc. Am. B*, Vol. 24, No. 10, Oct 2007, pp. 2721–2726.
- ⁸Guan, G., Arnold, S., and Otugen, V., “Temperature Measurements Using a Microoptical Sensor Based on Whispering Gallery Modes,” *AIAA Journal*, Vol. 44, No. 10, Oct 2006, pp. 2385–2389.
- ⁹Ayaz, U. K., Ioppolo, T., and Otugen, M. V., “Wall shear stress sensor based on the optical resonances of dielectric microspheres,” *Measurement Science and Technology*, Vol. 22, No. 7, 2011, pp. 075203.
- ¹⁰Ioppolo, T., Ayaz, U., and Otugen, M. V., “Tuning of whispering gallery modes of spherical resonators using an external electric field,” *Optics Express*, Vol. 17, No. 19, Jan 2009, pp. 16465.
- ¹¹Ioppolo, T., Otugen, M. V., and Marcis, K., “Magnetic field-induced excitation and optical detection of mechanical modes of microspheres,” *Journal of Applied Physics*, Vol. 107, No. 12, 2010, pp. 123115.
- ¹²Ioppolo, T. and Otugen, M. V., “Magnetorheological polydimethylsiloxane micro-optical resonator,” *Opt. Lett.*, Vol. 35, No. 12, Jun 2010, pp. 2037–2039.
- ¹³“Model TLB-6800 Vortex Plus(TM) Laser System,” 2014.
- ¹⁴Fourquette, D., Otugen, M., Larocque, L., Ritter, G., Meeusen, J., and Ioppolo, T., “Whispering-gallery-mode-based seismometer,” June 3 2014, US Patent 8,743,372.